Oral presentation | Incompressible/compressible/hypersonic flow
Incompressible/compressible/hypersonic flow-I
Wed. Jul 17, 2024 2:00 PM - 4:00 PM Room D

[8-D-04] Characteristics of optimal disturbances for hypersonic flows over blunt wedges

*Yifeng Chen[1], peixu Guo[1], jiaao hao[1], chihyung wen[1] （1. The Hong Kong Polytechnic University ）

Keywords: Optimal disturbance, Boundary layer, Entropy layer

Characteristics of optimal disturbances for hypersonic flows over blunt wedges

Chen Yifeng, Guo Peixu, Hao Jiaao, Wen Chihyung

The Hong Kong Polytechnic University

July/17/2024, Kobe

12th ICCFD

1.Background and Motivation

- When the nose Reynolds number exceeds a certain value, the transition was triggered **before the appearance of unstable modes**.

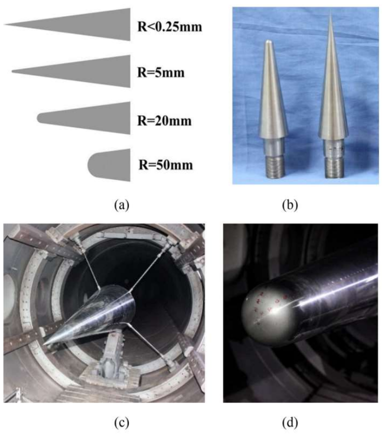

(Liu *et al.* PoF, 2022)

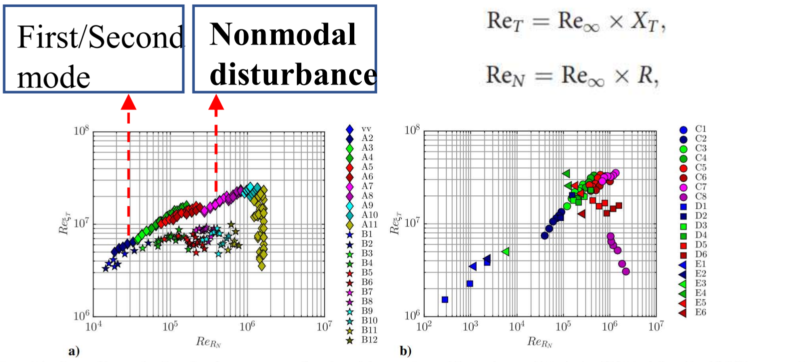

Fig. 1 Transition Reynolds number based on freestream as a function of the nose Reynolds number at a) Mach 6 and b) Mach 9 to 10, which illustrates the effect of bluntness and the transition reversal.

(Paredes *et al*, JSR, 2018, data A1-11 from Stetson AIAA 1983)

1.Background and Motivation

➢ PSD for blunt cones with different nose radius (R)

- High-frequency disturbances (Second mode)
- Low-frequency disturbances ?

(Paredes *et al.* Journal of Space and Rockets 2018)

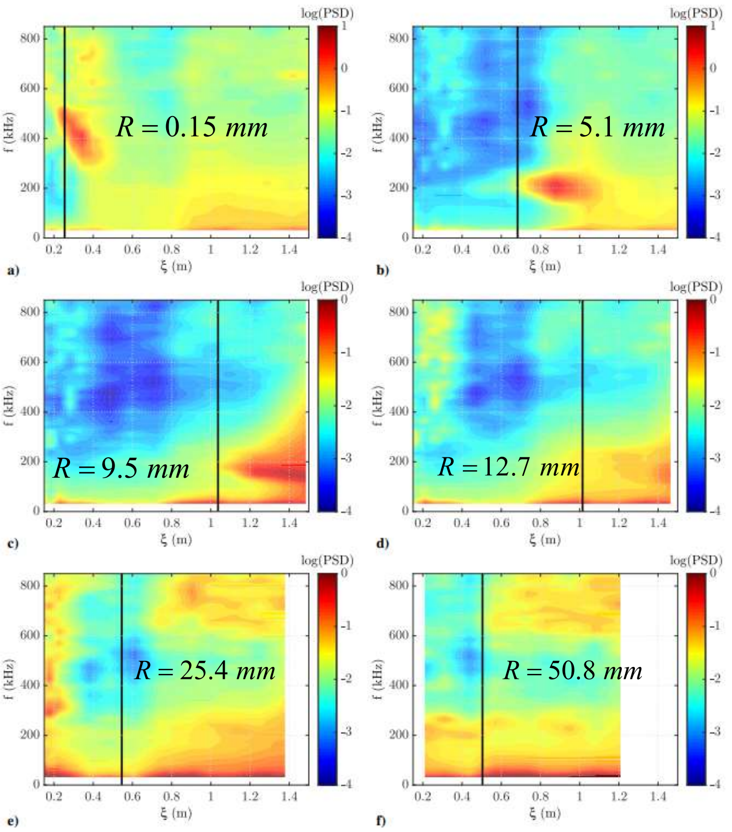

Solid black line: Transition location

1.Background and Motivation

- Wind tunnel experiment over blunt cones
  (Schlieren images)

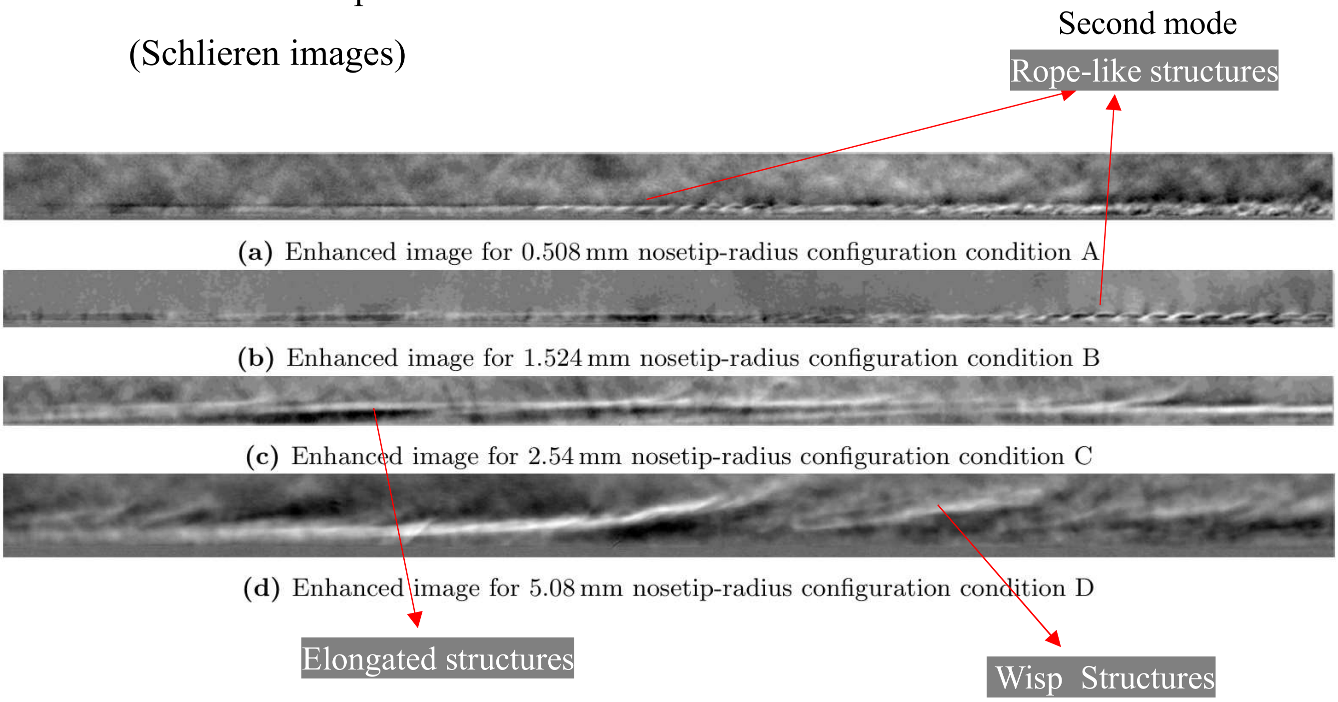

(a) Enhanced image for 0.508 mm nosetip-radius configuration condition A

(b) Enhanced image for 1.524 mm nosetip-radius configuration condition B

(c) Enhanced image for 2.54 mm nosetip-radius configuration condition C

(d) Enhanced image for 5.08 mm nosetip-radius configuration condition D

(Kennedy *et al.* AIAA 2019)

1.Background and Motivation

➢ **Blunt-tip Wedge - Research gap**

- Character of **optimal disturbances** (modal and nonmodal)
- The effect of **wall temperature**, **bluntness**
- Transient growth mechanism (**Orr/Lift-up mechanism**)
- **Entropy-layer** disturbances, **low-frequency** disturbances

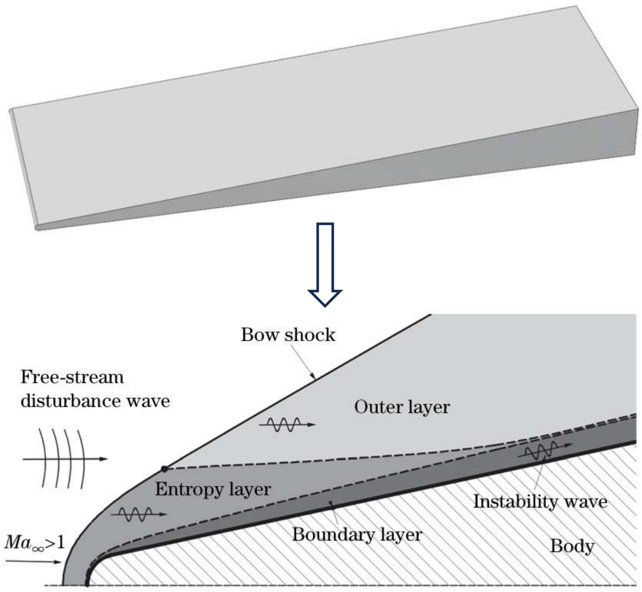

(Wan *et al.* AMM 2018)

2. Method-Stability analysis

➢ Resolvent analysis

$$\frac{\partial \boldsymbol{U}'}{\partial t}+\frac{\partial \boldsymbol{F}'}{\partial x}+\frac{\partial \boldsymbol{G}'}{\partial y}+\frac{\partial \boldsymbol{H}'}{\partial z}=\boldsymbol{0} \qquad \frac{\partial \boldsymbol{U}'}{\partial t}=\boldsymbol{A}\boldsymbol{U}'$$

$$\frac{\partial \boldsymbol{U}'}{\partial t}+\frac{\partial \boldsymbol{F}'}{\partial x}+\frac{\partial \boldsymbol{G}'}{\partial y}+\frac{\partial \boldsymbol{H}'}{\partial z}=\boldsymbol{B}\boldsymbol{f}'$$

$$\boldsymbol{f}'(x,y,z,t)=\hat{\boldsymbol{f}}(x,y)\exp(\mathrm{i}\beta z-\mathrm{i}\omega t)$$

$$\boldsymbol{U}'(x,y,z,t)=\hat{\boldsymbol{U}}(x,y)\exp(\mathrm{i}\beta z-\mathrm{i}\omega t)$$

$$\omega=\omega_r+\mathrm{i}\omega_i \qquad \hat{U}=\boldsymbol{R}\boldsymbol{B}\hat{\boldsymbol{f}}$$

- Resolvent matrix $\boldsymbol{R}=(-\omega_r\boldsymbol{I}-\boldsymbol{A})^{-1}$
- Optimal gain $\sigma^2(\beta,\omega_r)=\max_{\hat{f}}\frac{\|\hat{U}\|_E}{\|\boldsymbol{B}\hat{\boldsymbol{f}}\|_E}$

(Hao *et al.* JFM 2023)

➢ LST and LPSE

$$\boldsymbol{\psi}=(\rho,u,v,w,T)^{\mathrm{T}}$$

$$\boldsymbol{\psi}'(x,y,z,t)=\hat{\psi}(x,y)\exp\left(\mathrm{i}\int_{x_0}^{x}\alpha d\tilde{x}+\mathrm{i}\beta z-\mathrm{i}\omega t\right)$$

$$(\boldsymbol{\Gamma}_0+\boldsymbol{\Gamma}_1)\hat{\boldsymbol{\psi}}+\boldsymbol{\Gamma}_2\frac{\partial\hat{\boldsymbol{\psi}}}{\partial x}+\frac{\partial\alpha}{\partial x}\boldsymbol{\Gamma}_3\hat{\boldsymbol{\psi}}=\boldsymbol{0}.$$

LST ⇐ locally parallel flow | non-parallel base flow | non-local shape function | non-local streamwise wavenumber

(Guo *et al.* JFM 2023)

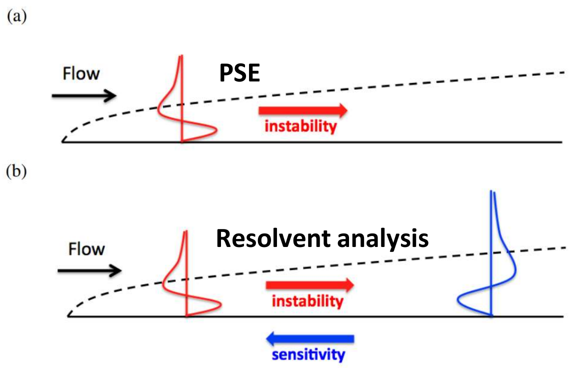

(Cook *et al*, AIAA 2018)

3. Model and flow parameters

$M_\infty = 5.9$ $\quad R = 2.54\ mm$ $\quad Re_\infty = 9.15\times10^7\ /\ m$ $\quad L^* = 1\ mm$ $\quad \theta = 5^o$

$T_\infty = 76.74K$ (Paredes *et al*, AIAA 2019)

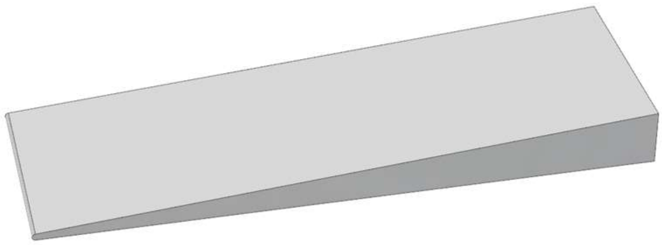

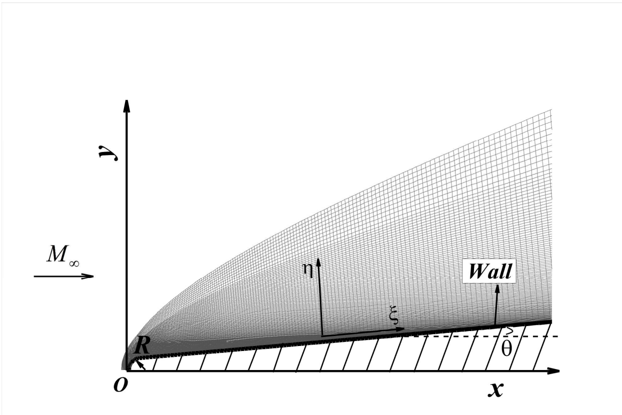

A schematic diagram of the computational model and coordinate systems.

4. Result - Base flow

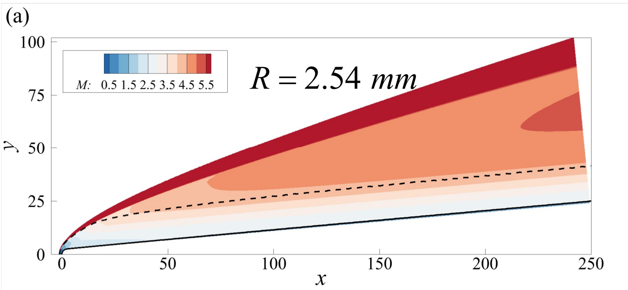

Dashed black line: Entropy-layer edge

Solid black line: Boundary-layer edge

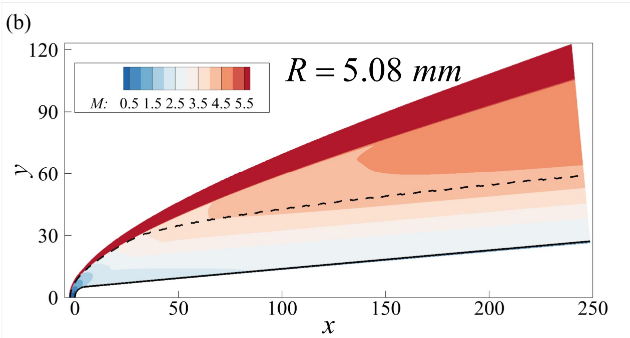

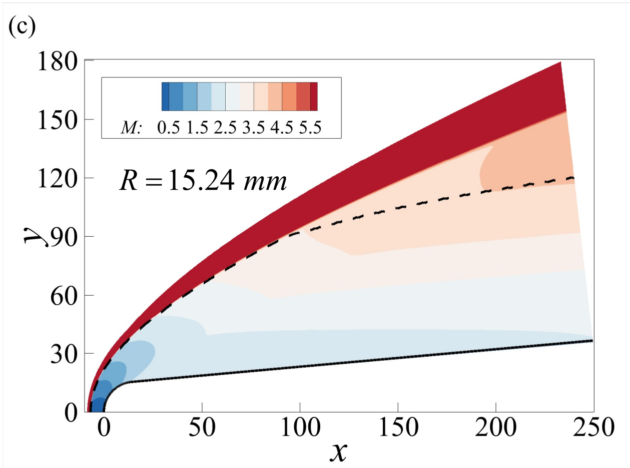

4. Result - Character of optimal responses

$R = 2.54\ mm$ $T_w / T_{ad} = 0.57$ $\omega = 0.3\ (f^* = 50\text{kHz})$ $N = 0.5\ln(E_{Chu} / E_{Chu,x_0})$

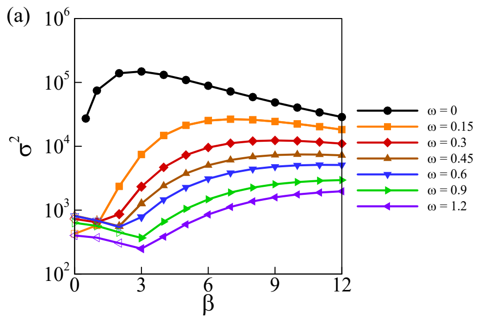

Pattern A (hollow symbols)
Pattern B (solid symbols)

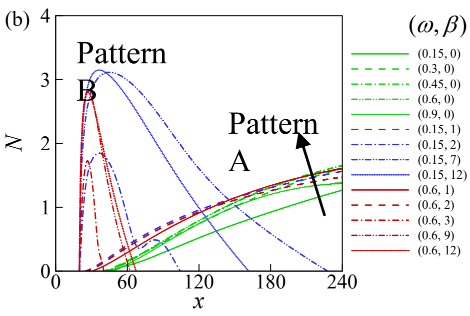

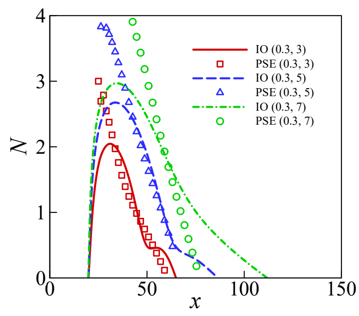

- Pattern A (disturbance inside the entropy layer)
- Pattern B (disturbance inside the boundary layer)

➢ Character of optimal response-Pattern A (plane wave)

$R = 2.54\ mm \qquad T_w / T_{ad} = 0.57$

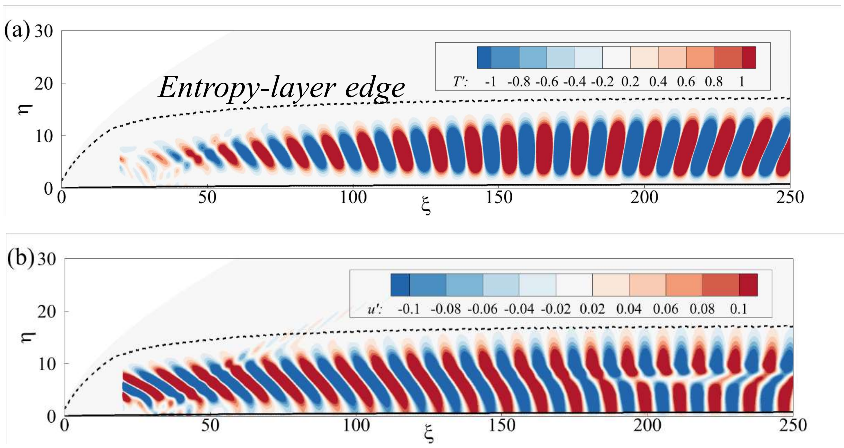

Contours of normalized (a) temperature and (b) streamwise velocity of optimal response for (0.45, 0)

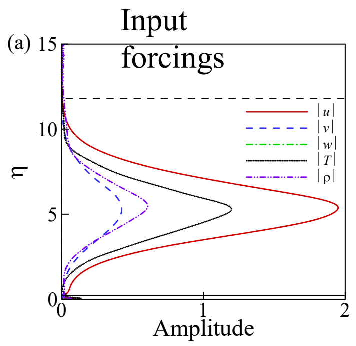

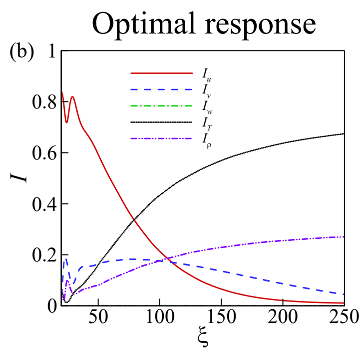

$$I_u(x) = \int_0^\infty \left(\bar{\rho} u'^2\right) dy \Big/ 2E_{Chu} \qquad E_{Chu}(x) = \frac{1}{2}\int_0^\infty \left[\bar{\rho}(u'^2 + v'^2 + w'^2) + \frac{\bar{T}}{\gamma Ma_\infty^2 \bar{\rho}}\rho'^2 + \frac{\bar{\rho}}{\gamma(\gamma-1)Ma_\infty^2 \bar{T}} T'^2\right] dy$$

➢ Character of optimal responses-Pattern B (streaks)

$R = 2.54\ mm \qquad T_w / T_{ad} = 0.57$

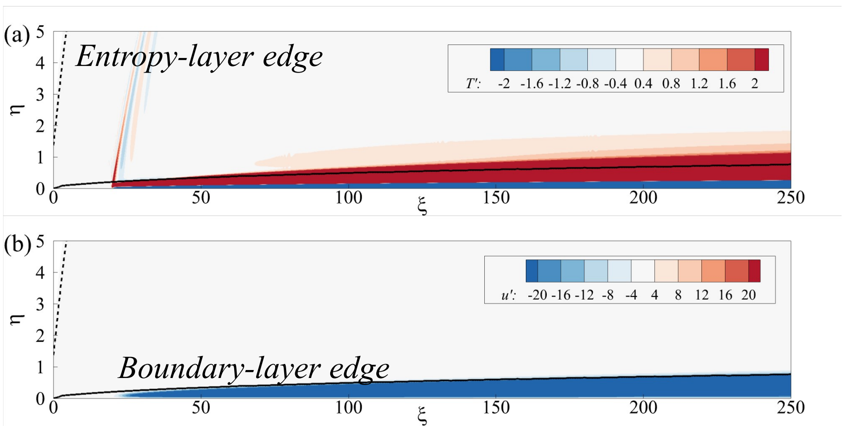

Contours of normalized (a) temperature and (b) streamwise velocity of optimal response for streaks (0, 2)

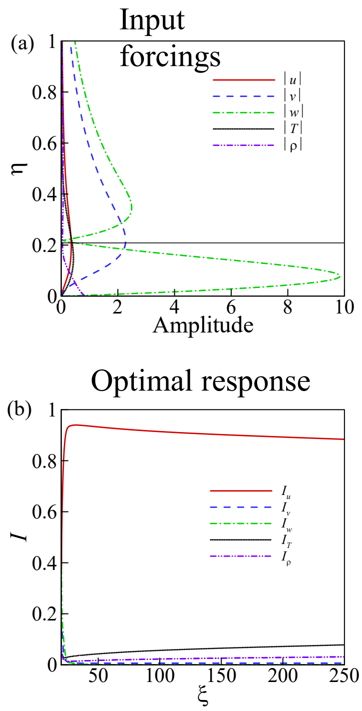

➢ Character of optimal responses-Pattern B (oblique wave)

$R = 2.54\ mm \qquad T_w/T_{ad} = 0.57$

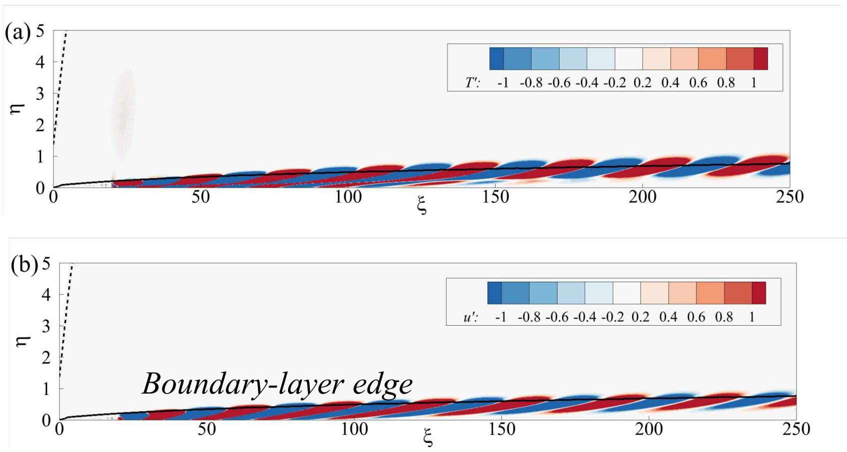

Contours of normalized (a) temperature and (b) streamwise velocity of optimal response for (0.3, 7)

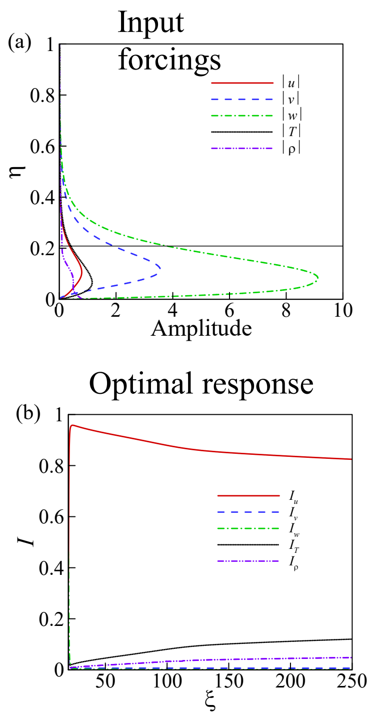

THE HONG KONG POLYTECHNIC UNIVERSITY 香港理工大學

➢ Effect of wall cooling

$$M = 5.9 \qquad R = 2.54\ mm$$

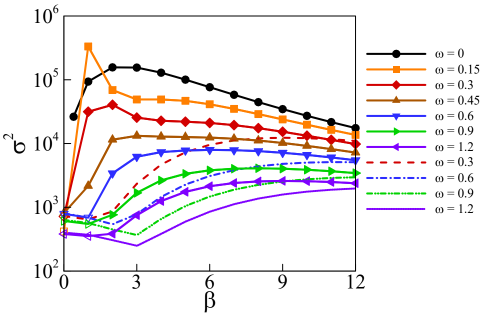

Adiabatic wall (solid line); Cold wall (dashed line)

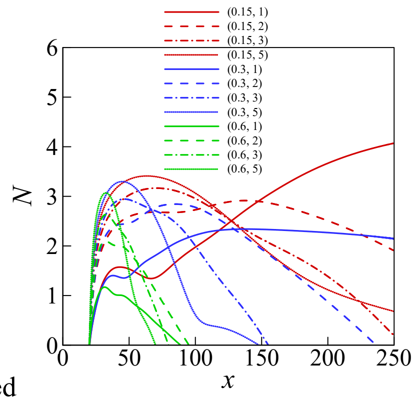

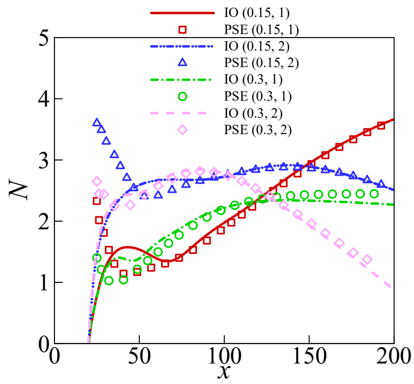

- Adiabatic wall leads to the appearance of **the first mode**.
- The energy gain of the first mode (0.15, 1) is largest among all ω and β
- Generally, wall cooling would lead to a **lower** energy gain

➢ Effect of wall cooling (R = 2.54 mm)

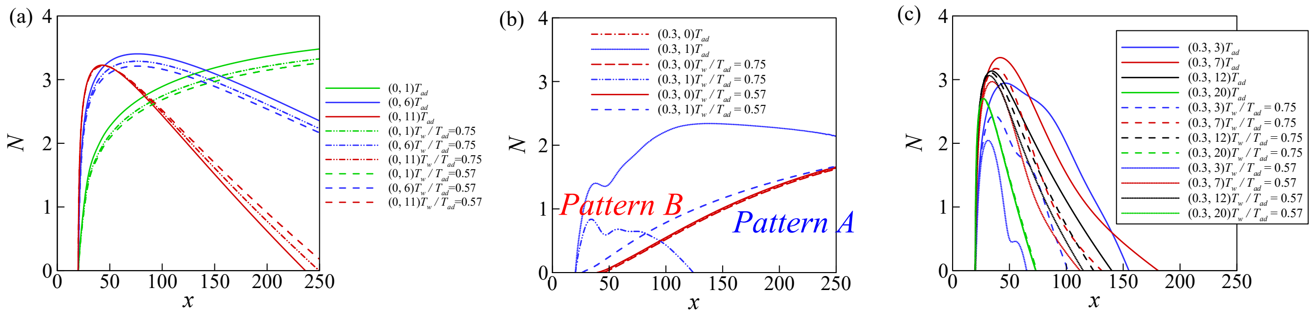

- Wall cooling has **no effect** on pattern-A disturbance
- Wall cooling would generally **weaken** pattern-B disturbance

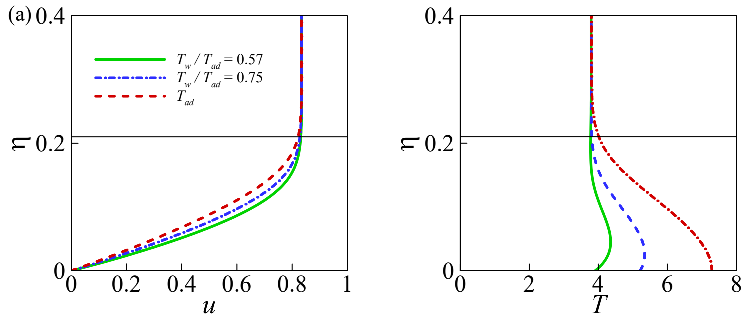

4. Result

➢ **Effect of bluntness** $R = 2.54\ mm$ $R = 5.08\ mm$ $R = 15.24\ mm$

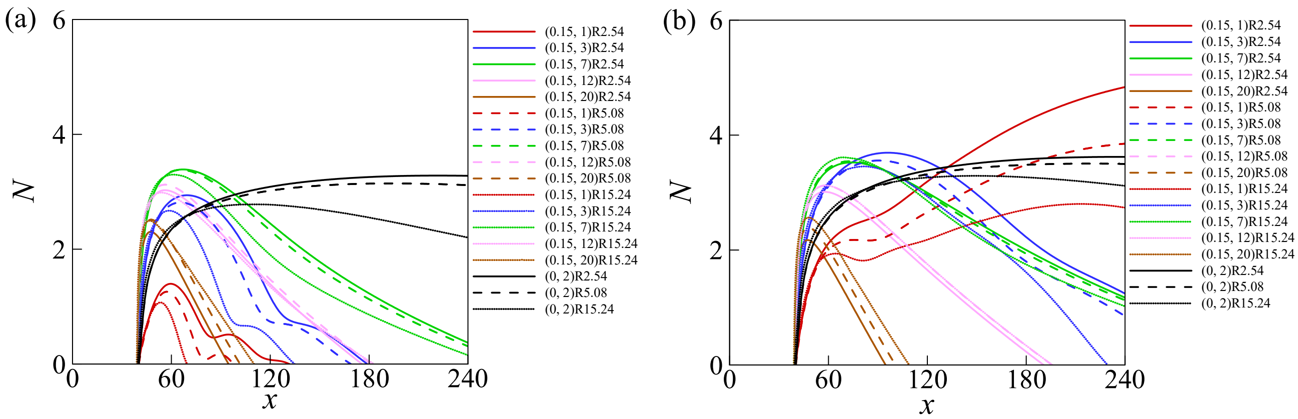

cold wall ($T_w / T_{ad} = 0.57$)

Adiabatic wall

- Generally, the increment of bluntness would lead to a **weaker modal and non-modal growth**

4. Result - Orr/Lift-up mechanism

➢ Vorticity components-Pattern A

$$(\omega,\ \beta) = (0.45,\ 1),\ \ T_w / T_{ad} = 0.57$$

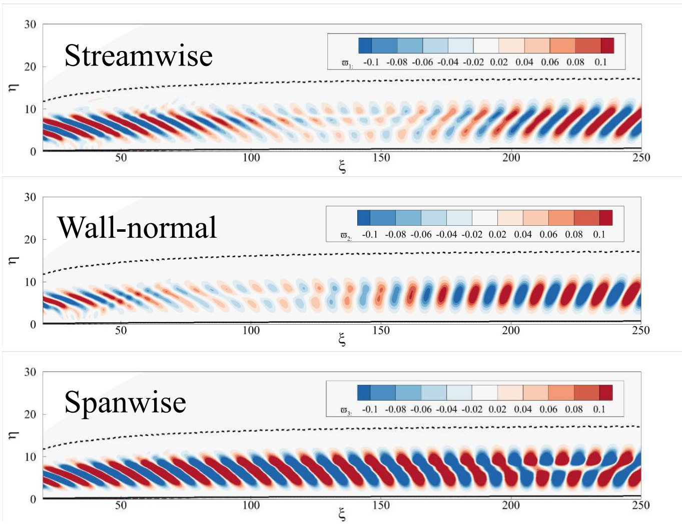

- Dominated by tilting in the shear direction (Extract energy from mean shear, **Orr mechanism**)

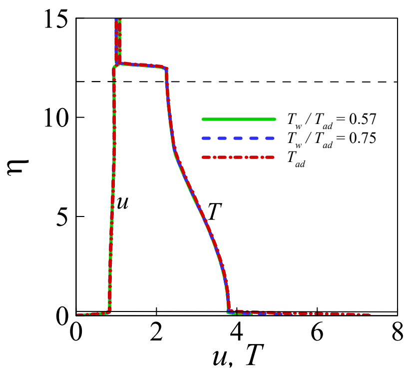

- Temperature gradient inside the entropy layer is **more evident** than that of streamwise velocity

➢ Orr/Lift-up mechanism

- *I* indicators of Chu energy components and Enstrophy ratios

$r_i(x) = \Omega_i / \sum_i \Omega_i \,,\ \Omega_i(x) = \int_0^{\infty} \varpi_i^2 dy$

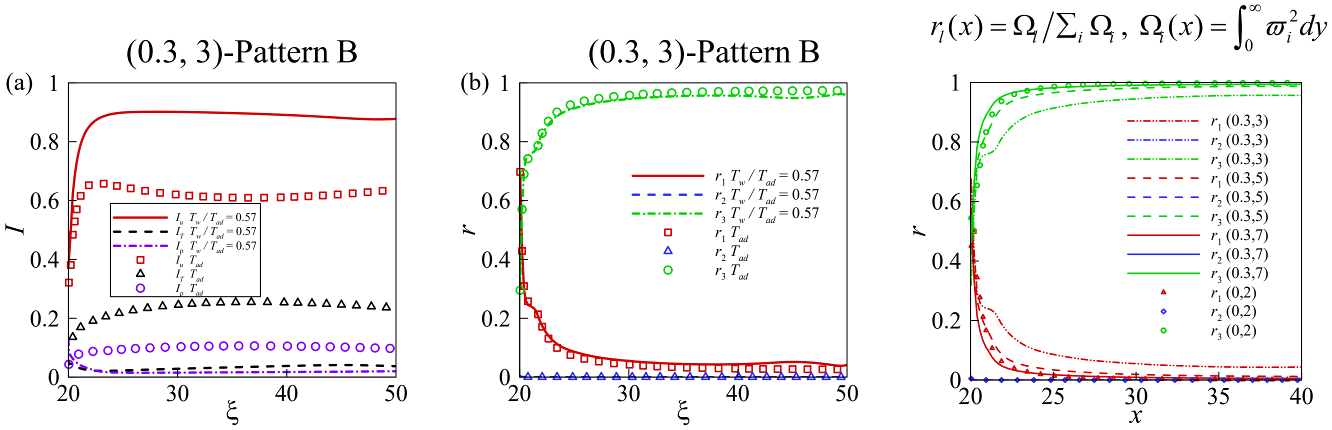

- Wall cooling has **no evident effect** on vorticity transfer
- **Weaker thermodynamic** energy-destabilization effect of wall cooling on pattern B

- Evolution of enstrophy ratios of (0.3, 7) **approaches** (0, 2)

➢ Competitive patterns

- **A demonstration case**

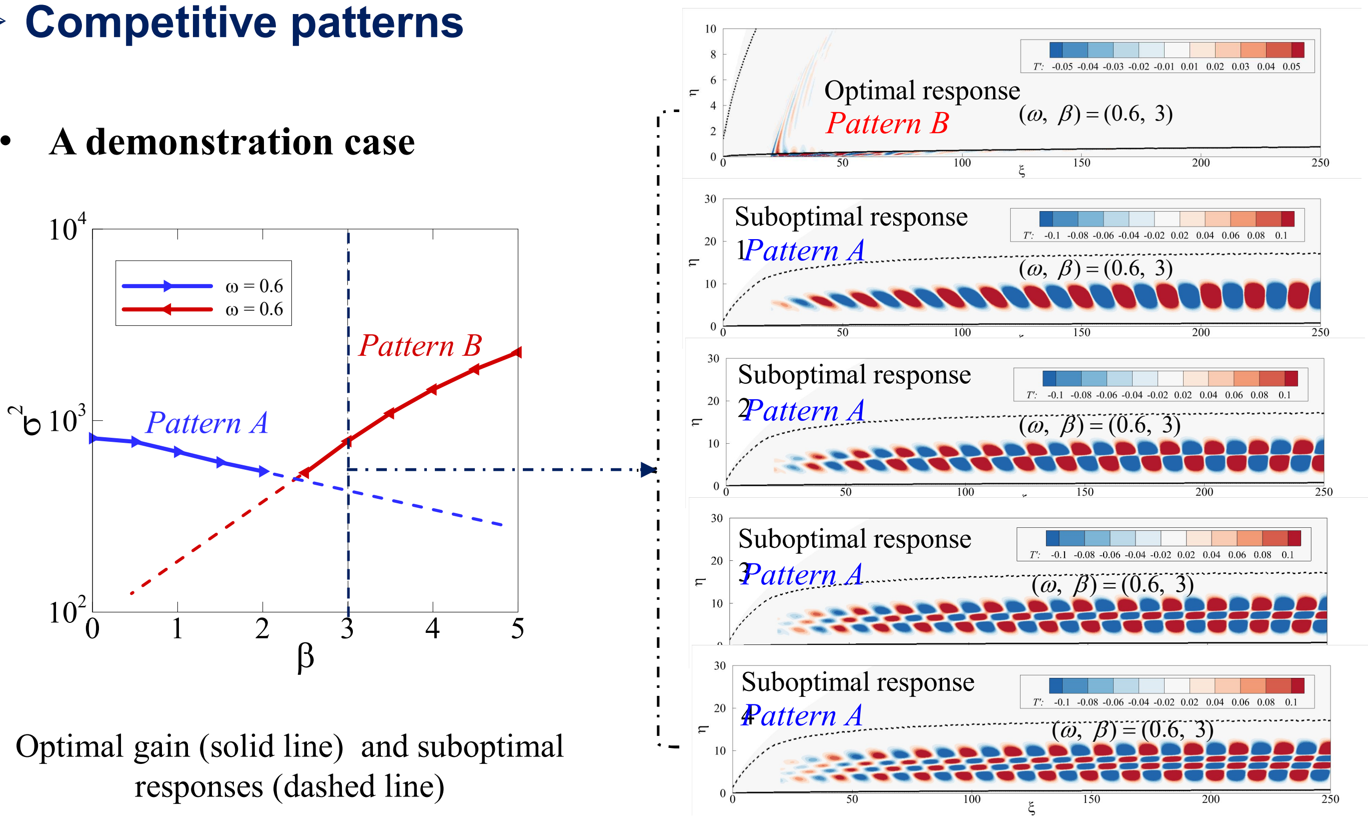

Optimal gain (solid line) and suboptimal responses (dashed line)

Similar structures

- Wind tunnel experiment over blunt cones

  (Schlieren images)

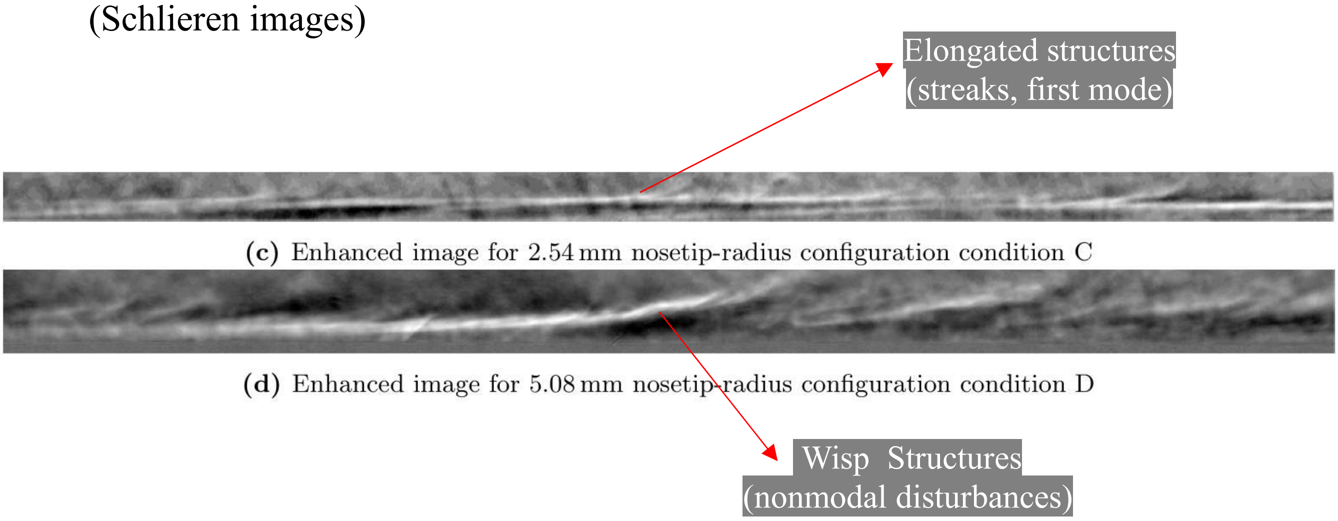

(c) Enhanced image for 2.54 mm nosetip-radius configuration condition C

(d) Enhanced image for 5.08 mm nosetip-radius configuration condition D

(Kennedy *et al.* AIAA 2019)

4. Result

➢ Competitive patterns-A demonstration case for (0.6, 3)

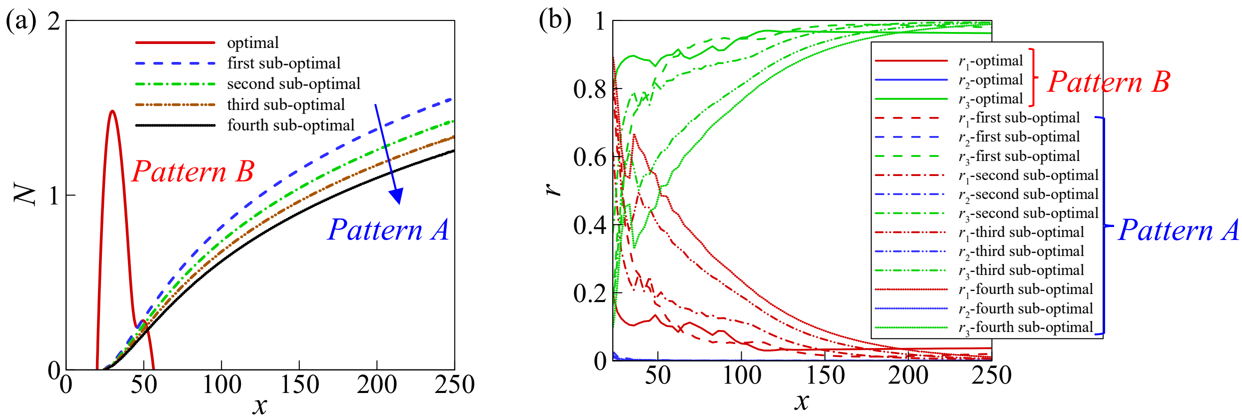

- Vorticity transfer is **more efficient** for optimal disturbance, followed by the first, second, third and fourth sub-optimal response

5. Summary

- **Competitive patterns** were identified by resolvent analysis
- Effect of wall cooling **depends on specific patterns**
- **No visible strengthening** of modal or non-modal growth when increasing bluntness
- **Both** Orr and Lift-up mechanisms may be involved in the transient growth

6. Potential future works

- Geometry of the leading edge (cylinder, ellipse…)
- Non-linear interaction between different growth patterns
- Transient growth near the nose
- Interaction between disturbance and the bow shock

THANKS!